IJISET - International Journal of Innovative Science, Engineering & Technology, Vol. 3 Issue 8, August 2016
ISSN (Online) 2348 – 7968 | Impact Factor (2015) - 4.332
www.ijiset.com

One Dimensional Mathematical Model of Bed-Load Sediment Transport In Shallow Water Flows

Amedeo Mwarania, Simon Mutugi

ABSTRACT

This mathematical modeling implements a strategy of using shallow water equations together with bed updating equation to analyze the changes of the bed topography. One dimensional Hyperbolic Partial Differential Equations are solved numerically. We present a class of numerical scheme called the relaxation scheme which combines finite volume shock capturing spatial discretization that is Riemann solver or nonlinear systems of algebraic equations solver free and Runge-kutta method that provide the time stepping mechanisms. Discretization for both spatial and time are carried separately using the method of lines. A second order MUSCL method discretizes the spatial derivative-semi discrete scheme and Runge-kutta time stepping mechanisms is used to discretize the time derivative in order to achieve fully discretized scheme of the hyperbolic problem to solve the system. The proposed schemes combine simplicity and high efficiency. The bed porosity will be varied on two bed geometry to realize the changes on bed topography and the water surface.
KEY TERMS: Conservation equation, Discretization, Shallow water equations

I. INTRODUCTION

A wide variety of physical phenomena are governed by STEs; an important class of practical problem of interest involves the water flow. As the water flows in natural rivers, man-made channels, in the seashore, through erosion or Tsunami; there is a subsequent change on the bed of that flow. Since these changes vary with different flows and different beds, a lot of research has been carried in various fields to investigate what exactly causes these changes of the bed. In the recent work numerical solutions for bed height has been obtained by varying physical parameters such as sediment transport flux (q) and nonnegative parameter A from the sediment transport flux relation $q(u) = Au^3$, without taking into consideration the effect of change of porosity on the bed. We were therefore motivated to determine the numerical solution for bed height by varying the porosity of the bed. In our study we investigated if the type of the bed has an impact on changes of the bed and consequently the water surface. It is obvious that as the water flows it carries with it some sediment; we will also study the effects of these sediments on the bed. We shall simulate shallow water equations and bed up-dating equations to analyze the changes.

Also from the observations of waves on the surface of water either on the sea or ocean and of the sediments and depositions after the flow, motivated us to investigate what made these occurrences to happen in the physical world. These two scenarios have been diagrammatically represented using figure 1 and 2 below respectively.

Figure 1: Waves on the surface of the water

In figure 1, water waves are seen moving forward and backwards. These waves keep varying in height progressively. There are also some portions of the surface where the flow is uniform.

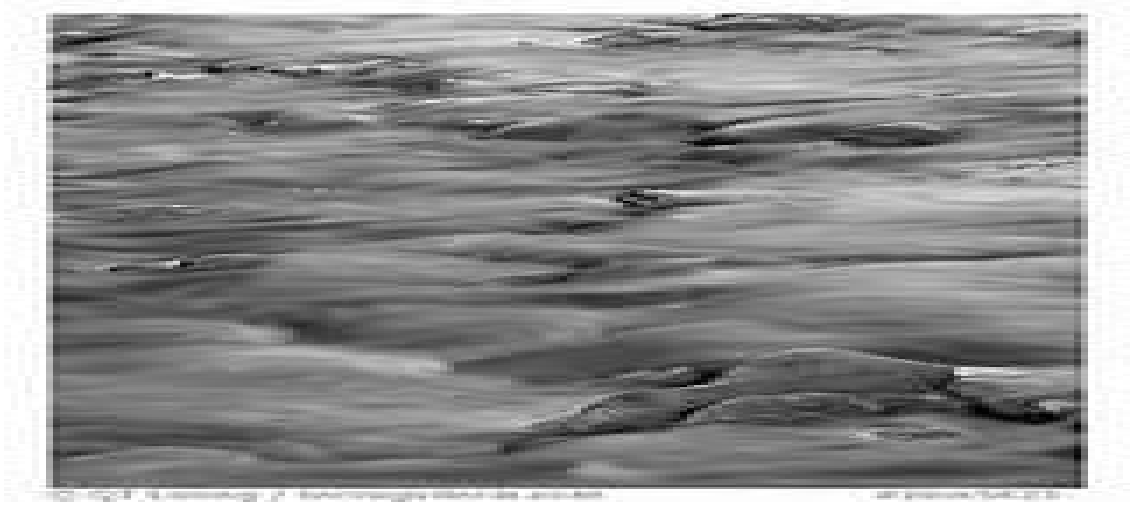

Figure 2: Sediments flow and deposition

Figure 2, shows sediment depositions on the bed of the sea. These depositions are non-uniformly distributed, and there are sections with no depositions but only pools of water.

Definition1: Incompressible fluid **refers to a fluid in which the material density is constant within a fluid parcel.**

Definition2: Inviscid fluid **(**In fluid mechanics) is a fluid which has no viscosity. It therefore can support no shearing stress and flows without energy dissipation. It is also known as ideal fluid, non-viscous or perfect fluid.

Definition3: Porosity is the measure of the void spaces in a material, and is a fraction of the volume of voids over the total volume and ranges between 0 and 1. There are two types of porosities; effective and ineffective. Ineffective (total) porosity includes both interconnected and isolated pore spaces while the effective include only the interconnected. Because only interconnected pores store and transmit fluids, we are mainly concerned with effective porosity.

Definition4:Relaxation scheme is a class of numerical schemes for solving conservation laws, that is hyperbolic or elliptic PDEs (JIN and XIN; 2002). They are developed for solving large sparse linear systems which arose as finite difference discretization of differential equations. Relaxation scheme has several advantages compared to schemes such as; Lax-Freidrichs scheme, classic Lax-Wendroff scheme, MacComark scheme, that is;

i. It overcomes the difficulties like spurious oscillations obtained from other methods like classic Lax-Wendroff and MacCormack schemes.
ii. It does not use Riemann problem solvers or nonlinear systems of algebraic equations solvers which takes more computational time during the solution process.
iii. Relaxation scheme in c-formulation is stable for long time calculations producing accurate and comparable results for small and relatively large Froude numbers.
iv. In multi-dimensions, relaxation schemes can be highly optimized for vectors computers since they do not require nonlinear procedures and contain no recursive elements.

In this study we are concerned with the application of numerical approximation known as relaxation scheme to sediment transport equations. The equations comprise the nonlinear shallow water equations governing the water flow with addition of bed

transport equation governing sediment transport forming a system of conservative laws.

These coupled systems of equations are numerically approximated to obtain the effect of changes of porosity on the bed topography and water surface. When there is fluid movement in rivers, channels and coastal areas there is a subsequent change on the bed topography due to flow and sediment movements. The porosity of the bed, the bed geometry, the height of the flow and the velocity of the flow mostly determines the changes on the bed topography. This numerical method does not utilize Riemann problem solvers or nonlinear iterations scheme hence making it to enjoy great simplicity in its approximation. This simplicity can be of great significance when one has to solve large scale engineering problems or has to calculate complicated Jacobian matrices that follow the use of complex fluxes (such as a sediment transport flux) .

In this paper we consider a coupled model constituted by hydrodynamic component and a morphodynamic component. The hydrodynamic component is modeled by SWEs which are used to study fluid movement in rivers, channels and coastal areas; while morphodynamic component is modeled by updating equation depending on solid transport flux. The central concern of morphodynamics is to determine the evolution of bed levels for hydrodynamic systems such as rivers, estuaries, inlets, bays and other near shore regions where fluid flows interact and induce significant changes to bed geometry.

Numerical morphological models involve coupling between a hydrodynamic model, which provides a description of the flow field leading to a specification of local sediment transport rates, and an equation for bed level change which expresses the conservative balance of sediment volume and its continual redistribution with time.

Transport of sediments is caused by gravity effects with the air or the fluid containing the sediment. Sediment transport is generally divided into three: bed load, saltation and suspension. Bed load transport is the transport where sediment grains roll or slide along the bed, while saltation is the type of transport where single grains jump over the bed a length proportional to their diameter, losing for instants the contact with the soil. Sediment is suspended when flux is intense enough such as the sediments grains reach height over the bed. In this work we shall not consider total transport since suspension and saltation transport give rise to other equations which will not be considered in this study. Hence the objective of this work is to demonstrate from

numerical point of view how variation of porosities on the bed changes the bed height and flow surface.

II. SHALLOW WATER EQUATIONS

Godunov (1959) suggested one of the methods to solve SWEs which involved Riemann solvers and aimed in getting the best solution around discontinuities. In this method, the space is discretized into cells and the fluxes are computed by solving Riemann problem at the interface (between cells). Godunov approach offers a treatment of discontinuities in hyperbolic system by assuming piecewise constant distribution of data within computational grid cells and solving the resultant discontinuities or Riemann problems that exist at each cell interface.

Gerald Blom *et al*. (2014) modeled sediment transport in shallow lakes using shallow water equations. Their simulation experiment was done in Lake Veluwe (Netherlands) in which model options with and without the distinction of sediment fractions were used, showing that using sediments fractions can account to variability in the sediment composition which leads to an improvement of the model results particularly the simulated phosphorus sediment water exchange fluxes.

Stoker (1957) in his work he concluded that SWEs represented a popular mathematical model for modeling free surface, flows arising in shores, rivers and so on. Due to nonlinearity of the model as well as the complexity of the geometry encountered in real life applications much effort has been made in recent years to develop numerical methods to solve the equations approximately.

Hirsch (1990) pointed out that for shock-capturing models; explicit schemes are typically used rather than implicit schemes. The weakness of explicit is due to restricted courant number but advantage is reducing in computing time.

Hudson (2001) proposed a variety of numerical scheme for approximating equations governing sediment transport which include adapted versions of the Lax-Freidrichs scheme, classic Lax-Wendroff scheme, MacComark scheme and Roe’s scheme. High

resolution schemes are also derived that satisfy the TVD property so that no spurious oscillations will occur in the numerical results. Five different formulations are then derived which are based on either a steady or unsteady approach and are used with the most accurate scheme and compared to determine which approach and numerical scheme is the most accurate. Sediment transport equations in both 1-D and 2-D are considered and dimensional splitting schemes are also discussed in two dimensions. It was noted that from the comparison; both in 1-D and 2-D, the adaptations of the flux-limited version of Roe's scheme produced very accurate numerical results.

i) Sediment transport and bed topography

Dung *et al*. (2014) studied large scale suspension sediment transport and sediment deposition in the Mekong Delta (Vietnam). The study presented a comprehensive approach to quantify suspended sediment and sediment related nutrient transport and deposition in the whole Mekong Delta. The model quantifies spatial and temporal variations of the suspended sediment transport and sediment –nutrient deposition from Kratie at the entrance of the Mekong to the coast. The model can be used to estimate the impact of the current and expected sea-level rise on the sediment transport in the Mekong Delta.

David (2004) studied numerical approximation of the non-linear shallow water equations with topography and dry beds using a Godunov Type scheme. In his work he realized Godunov Type method can successfully deal with difficulties such as discontinuities arising in hyperbolic PDEs such as the shallow water equations. Additionally it maintains positivity of the solution when confronted with very shallow flows and captures moving wet-dry fronts in the domain even over topography. By incorporating the source term directly into the Riemann solution it also preserves steady states. Because of these properties it is believed to be well suited for many realistic applications that present these difficulties.

Weng Long *et al*. (2007) on their paper Numerical Scheme for Morphological bed level calculations discussed several shock capturing schemes for simulating bed level change with different accuracy and stability behaviors. Their conclusion was in favor of a fifth order Euler WENO scheme which is introduced to sediment transport

simulations here over other schemes. The Euler WENO scheme is shown to have significant advantages over other schemes with artificial viscosity and filtering processes, hence is highly recommended especially for phase-resolving sediment transport models.

ii) RELAXATION SCHEME

Delis and Katsaounis (2003) studied relaxation scheme for the shallow water equation in one dimension with and without topography source term. They established that the main feature of the schemes is their simplicity and robustness. Finite volume shocks capturing spatial discretization that are Riemann Solver free have been used providing accurate shock resolution. A new way to incorporate the topography source term was applied with the relaxation model and only small errors were introduced while preserving steady states. The bench tests show that the schemes provide accurate solutions in agreement with well known analytical solutions. The results also demonstrates that relaxation schemes are accurate, simple, efficient and robust and can be of practical consideration when solving shallow water flow problems involving bed slope source terms.

Delis and Papoglou (2007) proposes and applied a numerical method based on finite volume relaxation approximation for computing the bed-load sediment transport in shallow water flows in one and two space dimensions. The water flow is modeled by well known nonlinear shallow water equations which are coupled with a bed-updating equation. Using a relaxation approximation the nonlinear set of equations (and for two different formulations) is transformed to a semi linear diagonalizable problem with linear characteristics variables. A second order MUSCL-TVD method is used for the advection stage while an implicit –explicit Runge-Kutta scheme solves the relaxation stage. In their work they varied physical parameters A and q from sediment transport flux $q(u) = Au^3$ to obtain different problem.

They concluded that the advantages of this approach are that neither Riemann problem solver nor non-linear iterations are required during the solution process. They tested the applicability and effectiveness of the scheme by comparing numerical results obtained for several bench mark test problems.

iii) MUSCL-SCHEME

The term MUSCL was introduced in a seminar paper by Bram Van Leer (1979). In his paper he constructed the first higher order Total Variation Diminishing scheme where he obtained second order spatial accuracy. The ideal was to replace the piecewise constant approximation of Godunov`s schemes by reconstructed states, derived from cell-averaged states obtained from the previous time-step. For each cell, slope limited reconstructed left and right states are obtained and used to calculate fluxes at the cell boundaries. These fluxes can in turn be used as input to a Riemann solver, following which the solutions are averaged and used to advance the solution in time. Alternatively the fluxes can be used in Riemann solver free scheme.

Ambrosi (1995) studied a TVD version of the Lax-Wendroff scheme in inviscid shallow water equations. Performance of the scheme is shown in 1-D and 2-D computations. He resolved two specific difficulties using the scheme that is; capability of the class of the scheme to handle geometric source that arise to model the bottom and situations in which strict hyperbolicity is lost when the eigenvalues collapses into one. He uses Roe's approximate Riemann solver enhanced by a slope limiting of MUSCL type scheme which combines two-order accuracy in time if the solution is smooth with the capability to compute discontinuities sharply and monotonically as standard first order scheme do.

Toro (2001) suggested that since most higher order linear schemes produced spurious oscillations they calls for MUSCL approach which is obtained by data reconstruction and reconstruction is constrained so as to avoid spurious oscillation and this justifies the word monotone in the scheme.
Our study shall utilize relaxation numerical scheme and the c-formulation of governing equations to analyze how change of porosity and sediment transport changes the bed topography and water surface.

III. DERIVATION OF SEDIMENT TRANSPORT EQUATIONS (STE'S)

Mass and momentum conservation equation are deduced by averaging Navier- Stokes equation under the hypothesis of hydrostatic pressure and small vertical variations of the velocity. The unknowns $h(x,t)$ is the total height above the bottom of the

channel, $B(x,t)$ is the height of the bed topography function, $u(x,t)$ velocity of the river in the x-direction, $\eta(x,t)$ surface elevation and $q(u,h)$ is the bed load volumetric sediment transport rate in the x-direction.

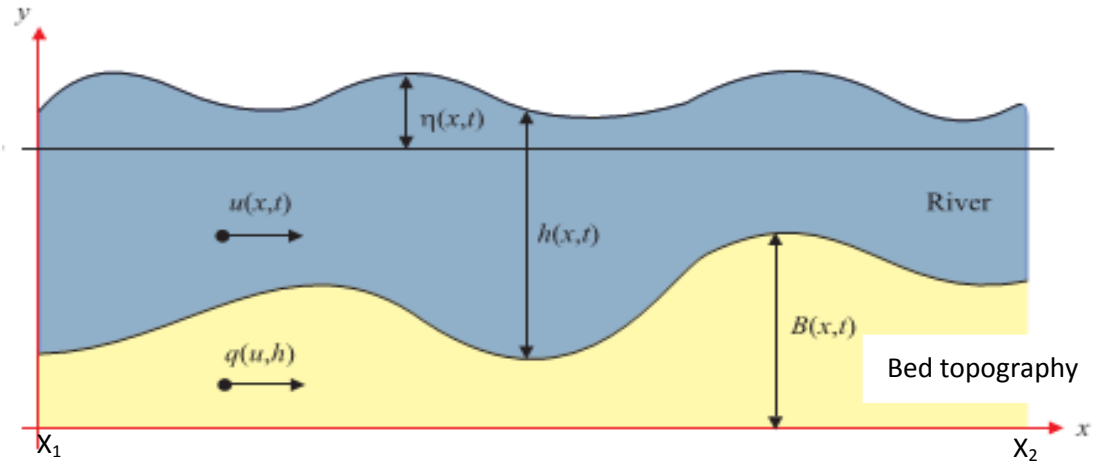

Figure 3: shallow water domain

We discuss the derivation of the equations governing sediment transport together with two alternatives sediment transport flux formulae. We first derive the equations that govern fluid with sediment transport from the basic conservation laws.

In our derivation, the following assumptions will be observed:

i. The fluid (water) is incompressible.
ii. Water motion is unsteady with respect to changes in bed level.
iii. Fluid flow is moving in x-direction.
iv. There is no effect of variation of channel width on the bed topography.
v. There is no effect of friction and pressure on the bottom and on the surface of the flow.

By considering a region between x_1 and x_2 , in the one dimensional channel illustrated in figure 1. We can derive the equations governing sediment transport.

i) Mass conservation equation

In the region x_1 and x_2, we can determine that,

$$\begin{bmatrix} \textit{net}\text{ volume of fluid into} \\ \text{the region } x_1 \text{ to } x_2 \end{bmatrix} = \begin{bmatrix} \text{rate of change of total volume} \\ \text{of fluid in the region } x_1 \text{ to } x_2 \end{bmatrix}.$$

Now the total volume of fluid in the region x_1 and x_2

$$\int_{x_1}^{x_2}\int_{B}^{h+B} dy dx = \int_{x}^{x_2} (h+B-B)dx = \int_{x_1}^{x_2} h dx \;\ldots\ldots\ldots\ldots\ldots\ldots\ldots\ldots\ldots\ldots\ldots\ldots\ldots\ldots (1)$$

and by differentiating with respect to t, we obtain

$$\begin{bmatrix} \text{rate of change of total volume of} \\ \text{fluid in the region } x_1 \text{to } x_2 \end{bmatrix} = \frac{d}{dt}\int_{x1}^{x2} h dx.$$

Also $\begin{bmatrix} \text{total volume of fluid} \\ \text{entering at } x_1 \end{bmatrix} = (uh)_{x1}$,

and $\begin{bmatrix} \text{Total volume of} \\ \text{fluid leaving at } x_2 \end{bmatrix} = (uh)_{x2}$.

Thus $\begin{bmatrix} \text{net volume of fluid} \\ \text{into region } x_1 \text{ to } x_2 \end{bmatrix} = (uh)_{x1} - (uh)_{x2}$

$$\frac{d}{dt}\int_{x_1}^{x_2} h dx + [uh] = 0 \;\ldots\ldots\ldots\ldots\ldots\ldots\ldots\ldots\ldots\ldots\ldots\ldots\ldots\ldots\ldots\ldots (2)$$

To obtain the differential form we integrate above with respect to t over the interval $[t_1 \text{ to } t_2]$, where $[t_2 > t_1]$

$$\int_{x_1}^{x_2} h(x,t_2)dx - \int_{x_1}^{x_2} h(x,t_1)dx + \int_{t_1}^{t_2} [uh]_{x_1}^{x_2}\, dt = 0.$$

Then by assuming that $h(x,t)$ and $u(x,t)$ are differentiable functions and using

$h(x,t_2) - h(x,t_1) = \int \frac{\partial h}{\partial t} dt$ and

$$[uh]_{x1}^{x2} = \int_{x1}^{x2} \frac{\partial (uh)}{\partial x} dx$$

we obtain

$$\int_{t_1}^{t_2}\int_{x_1}^{x_2}\left\{\frac{\partial h}{\partial t}+\frac{\partial(uh)}{\partial x}\right\}dxdt=0 \quad \text{.....(3)}$$

Since x_1 and x_2 and t_1 and t_2 are arbitrary, we obtain the differential form of equation for conservation of mass in one dimension as;

$$\frac{\partial h}{\partial t}+\frac{\partial(uh)}{\partial x}=0. \quad \text{……..……..……...…... (4)}$$

ii) Conservation of momentum

Applying Newton second law (N_2L) of motion, in the region x_1 and x_2 we determine that

$$\begin{bmatrix} total \text{ rate of change of} \\ \text{momentum in x - direction} \end{bmatrix}=\begin{bmatrix} force \text{ applied} \\ \text{in x - direction} \end{bmatrix}.$$

Now,

$$\begin{bmatrix} Total \text{ rate of change of} \\ \text{momentum in x - direction} \end{bmatrix}=\frac{d}{dt}\int_{x_1}^{x_2}\int_{B}^{h+B} udydx+(hu^2)_{x_2}-(hu^2)_{x_1}=\frac{d}{dt}\int_{x_1}^{x_2} uhdx+(hu^2)_{x_2}-(hu^2)_{x_1}.$$

……..... (5)

Also,

$$[pressure \text{ force on ends}]=g\left[\int_{B}^{h+B}(y-(h+B))dy\right]_{x1}^{x2}=g\left[\left(\frac{1}{2}y^2-(h+B)y\right)_{B}^{h+B}\right]_{x_1}^{x_2}=\left[-\frac{1}{2}gh^2\right]_{x_1}^{x_2}$$

and

$$[pressure \text{ force from riverbed}]=-g\int_{C_{B1,2}} hdy,$$

where $C_{B1,2}$ is the path of the line integral and denotes the curve of the riverbed in the region, $x_1 to\ x_2$ by assuming that no discontinuities are present in the riverbed,

$$[pressure \text{ force from riverbed}]=-g\int_{x1}^{x2} h\frac{dB}{dx}dx,$$

we obtain,

$$[force \text{ applied in x - direction}]=\left[-\frac{1}{2}gh^2\right]_{x1}^{x2}-g\int_{x1}^{x2} h\frac{dB}{dx}dx. \quad \text{……..…... (6)}$$

Hence,

$$\frac{d}{dt}\int_{x_1}^{x_2} uhdx + (hu^2)_{x_2} - (hu^2)_{x_1} = \left[-\frac{1}{2}gh^2\right]_{x_1}^{x_2} - g\int_{x_1}^{x_2} h\frac{dB}{dx}dx, \quad \text{..... (7)}$$

and by re-arranging we obtain the integral form of the equation for conservation of momentum,

$$\frac{d}{dt}\int_{x_1}^{x_2} uhdx + \left[hu^2 + \frac{1}{2}gh^2\right]_{x_1}^{x_2} = -g\int_{x_1}^{x_2} h\frac{dB}{dx}dx. \quad \text{..... (8)}$$

To obtain the differential form of the equation for conservation of momentum in one dimension, we use the same approach as we did for the equation for conservation of mass and assume that $h(x,t)$ and $u(x,t)$ are differential functions and obtain

$$\frac{\partial uh}{\partial t} + \frac{\partial(hu^2 + \frac{1}{2}gh^2)}{\partial x} = -ghB_x \quad \text{..... (9)}$$

iii) Bed updating equation

In the $x_1 to\ x_2$ region we can determine that,

$$\begin{bmatrix} net \text{ flux of mass} \\ \text{into the region } x_1 \text{ to } x_2 \end{bmatrix} = \begin{bmatrix} rate \text{ of change of total} \\ \text{mass in the region } x_1 \text{ to } x_2 \end{bmatrix}$$

Now, the total volume of sediment in the region $x_1 to\ x_2$ is

$$\int_{x_1}^{x_2}\int_{0}^{B} dydx = \int_{x_1}^{x_2} Bdx \quad \text{..... (10)}$$

and by differentiating with respect to t, we obtain,

$$\begin{bmatrix} rate \text{ of change of} \\ \text{total mass in the region } x_1 \text{ to } x_2 \end{bmatrix} = \frac{d}{dt}\int_{x_1}^{x_2} Bdt.$$

In addition we have,

$$\begin{bmatrix} total \text{ volume of sediment} \\ \text{entering at } x_1 \end{bmatrix} = \xi q(u,h)_{x1}$$

and

$$\begin{bmatrix} total \text{ volume of sediment} \\ \text{leaving at } x_2 \end{bmatrix} = \xi q(u,h)_{x2}$$

Where $\xi = \frac{1}{1-\sigma}$ and σ is the porosity of the bed material, which is non-dimensional, with $0 \le \sigma < 1$, see Cunge *et al*.

Thus

$$\begin{bmatrix} net \text{ flux of mass into} \\ \text{the region } x_1 \text{ to } x_2 \end{bmatrix} = \xi(q(u,h)_{x1} - q(u,h)_{x2}).$$

Hence we obtain the integral form of the bed-updating equation,

$$\frac{d}{dt}\int Bdt + \xi[q(u,h)]_{x1}^{x2} = 0. \quad \text{..... (11)}$$

To obtain the differential form of the bed-updating equation, we use the same approach as we did for the equation for conservation of mass and momentum and assume that $h(x,t)$ and $u(x,t)$ are differentiable functions and obtain;

$$\frac{\partial B}{\partial t} + \xi\frac{\partial q}{\partial x} = 0 \text{ ..... (12)}$$

iv) Sediment transport flux formulae

The total load sediment transport flux includes saltation, bed load and suspended. Bed load transport is the transport where sediment grains roll or slide along the bed, while saltation is the type of transport where single grains jump over the bed a length proportional to their diameter losing for instants the contact with the soil/bed. Sediment is suspended when the flux is intense enough such as the sediments grains reach height over the bed. For slow water saltation and bed load sediment transport is more dominant as not much sediment is carried by the water flow but as the water flow increases, suspended sediment transport becomes more dominant and sediment can be transported several metres above the bed especially if the grain size is small. In this study we consider slow water and hence we do not consider suspended saltation sediment transport.

Numerous analytical sediment transport flux formulae have been derived that include saltation, bed load and suspended. Sediment transport and the choice of which to use is usually determined by the situation being modeled. We first consider two of the well known sediment transport flux formulae.

Grass (1981), discussed one of the most basic sediment transport fluxes which follow a simple power law.

$$q(u) = Au|u|^{m-1} \quad \text{(13)}$$

here A is a dimensional constant that encompasses the effect of grain size and kinematic viscosity and usually determined from experimental data with m being chosen so that $1 \le m \le 4$ .Unless u is not allowed to change sign, equation (13) cannot be differentiated with respect to u. However by considering odd integer values of m only, equation (13) can be differentiated and is valid for all values of u, for example, if we let $m = 3$ then,

$$q(u) = Au|u^2| = Au^3, \quad \text{(14)}$$

can now be differentiated with respect to u and is valid for all values of u

Van Rijn (1984), derived a more complex sediment transport flux,

$$q(u,h) = \begin{cases} Au\,(|u| - u_{cr})^{2.4}, & \text{if } |u| > u_{cr} \\ 0, & \text{otherwise} \end{cases} \quad \text{(15)}$$

where u_{cr} is the threshold current speed.

In this work we shall utilize discharge flux $q(u)$ from Grass (1981), which is more basic and can be applied with a wide range of velocity and the height of water.

To ensure the error of numerical scheme do not grow; the variables are non-dimensionalised

$$x^* = \frac{x}{L}, \quad t^* = \frac{t}{T}, \quad h^* = \frac{h}{L}, \quad B^* = \frac{B}{L}, \quad g^* = \frac{gT^2}{L}, \quad u^* = \frac{uT}{L}, \quad A^* = \frac{AL}{T^2}$$

Where L=100 and $T = \sqrt{\frac{100}{g}}$ are the non-dimensionalised coefficients and L is taken as the length of the channel.

Since $B(x,t)$ is an unknown, the model equations (4), (9) and (12) can be written in coupled form as;

$$\begin{bmatrix} h \\ hu \\ B \end{bmatrix}_t + \begin{bmatrix} hu \\ hu^2 + \frac{1}{2}gh^2 \\ \xi q \end{bmatrix}_x = \begin{bmatrix} 0 \\ -ghB_x \\ 0 \end{bmatrix} \quad \text{(16)}$$

where $\begin{bmatrix} 0 & -ghB_x & 0 \end{bmatrix}^T$ is inhomogeneous source term.

By using the product rule,

$$(hB)_x = h_x B + B_x h,$$

we can rewrite the source term obtaining as;

$$\begin{bmatrix} h \\ hu \\ B \end{bmatrix}_t + \begin{bmatrix} hu \\ hu^2 + \frac{1}{2}gh^2 + ghB \\ \xi q \end{bmatrix}_x = \begin{bmatrix} 0 \\ gBh_x \\ 0 \end{bmatrix} \quad \text{..... (17)}$$

Equation (17) is referred to as the C-Formulation (Hudson (2001)) because it is written in conservative variable form and whose Jacobian matrix is not singular.

For the C-formulation the Jacobian matrix is

$$J_c = \begin{bmatrix} 0 & 1 & 0 \\ g(h+B) - u^2 & 2u & gh \\ -ud & d & 0 \end{bmatrix},$$

where $d = (\frac{\xi}{h}) Am|u|^{m-1}$.

The matrix J_c is nonsingular with real and different eigenvalues which can be evaluated from the characteristic polynomial,

$$p(\lambda, \mathrm{w}) = \lambda^3 - 2u\lambda^2 + (u^2 - g(h + B + hd))\lambda + ghud = 0. \quad \text{..... (18)}$$

The eigenvalues are always real and unequal if $h(x,t) + B(x,t) > 0$ and represent the speed at which information propagates. The eigenvalue for fixed bed (no sediment transport; A=0 which implies d=0) is $\lambda = u \pm \sqrt{-g(h+B)}$.

For sediment transport where $\mathrm{A} \neq 0$ there are three speeds for the C-formulation; according to Hudson and Sweby (2003) the eigenvalues of equation (18) are;

$$\lambda_1 = 2\sqrt{-Q}\cos(\frac{1}{3}\theta) - \frac{1}{3}a_1,$$

$$\lambda_2 = 2\sqrt{-Q}\cos(\frac{1}{3}(\theta + 2\pi)) - \frac{1}{3}a_1,$$

and

$$\lambda_3 = 2\sqrt{-Q}\cos(\frac{1}{3}(\theta + 4\pi)) - \frac{1}{3}a_1$$

where $\theta = \arccos\frac{R}{\sqrt{-Q^3}}$,

$Q = -\frac{1}{9}(u^2 + 3g(h + B + hd))$,

and $R = -\frac{u}{54}(2u^2 - 9g(2h + 2B - hd))$

from equation (18) we establish that, $a_1 = -2u$.

IV. METHOD OF SOLUTION

Sediment transport equations are hyperbolic nonlinear partial differential equations .We will use relaxation scheme with MUSCL flux limiter method. To describe this method we first relax the system, secondly we discretize the equation in the relaxed system using the monotone upstream-centered scheme for conservation laws (MUSCL –scheme) to the semi-discrete relaxed scheme. This is also carried out using the method of lines where one variable (spatial domain) is discretized at first. Then in the final step of improving the result we carry out the full discretization using the second order TVD implicit Runge-kutta scheme to discretize the time variable.

a) RELAXATION SYSTEMS FOR SEDIMENT TRANSPORT EQUATIONS

Motivation of writing the relaxation systems of the sediment transport equations is borrowed from the relaxation system of the 1-D scalar conservation. For classical one dimensional conservation law.

$$\left.\begin{array}{l} u_t + f(u)_x = 0 \\ u(x,0) = u_0(x), \end{array}\right\} x\in\mathbb{R}, t>0 \quad \text{………………………………………………... (19)}$$

Equation (19) is initial value problem and Jin and Xin (2002) relaxed the above system as follow:

$$u_t + v_x = 0 \quad \text{…………………………………………………………………..……. (20a)}$$

$$v_t + c^2 u_x = -\frac{1}{\varepsilon}(v - f(u)) \quad \text{……………...……………………………………….. (20b)}$$

Where ε is the relaxation rate and c^2 is a positive constant describing the characteristic speed of the gravity wave and satisfying the stability criterion below,

$-c \le f'(u) \le c$, $\forall$ u. If the sub-characteristic condition $|f(u)| < c$ holds true then in the relaxation limit $\varepsilon \to 0$ we recover equation (19).

Following the above motivation, we write a relaxation system for the sediment transport equations replacing the conservation law by a larger system that is with $Q = hu$, equation (4) becomes;

$$h_t + Q_x = 0$$

Introducing variable v such that $v \to Q$ as $\varepsilon \to 0$ in $\frac{1}{\varepsilon}(v - Q)$

$$h_t + v_x = 0 \quad \text{..... (21a)}$$

$$v_t + c_1^{\,2} h_x = -\frac{1}{\varepsilon}(v - Q) \quad \text{..... (21b)}$$

Similarly equation (9) becomes $Q_t + (\frac{Q^2}{h} + \frac{g}{2}h^2)_x = -ghB_x$

Introducing variable w in the above equation such that $w \to (\frac{Q^2}{h} + \frac{g}{2}h^2)$ as $\varepsilon \to 0$ in $\frac{1}{\varepsilon}(w - (\frac{Q^2}{h} + \frac{g}{2}h^2))$, we obtain

$$Q_t + w_x = -ghB_x \quad \text{..... (22a)}$$

$$w_t + c_2^{\,2} Q_x = -\frac{1}{\varepsilon}\{w - (\frac{Q^2}{h} + \frac{g}{2}h^2)\} + \int^x gh(y)B'(y)dy \quad \text{..... (22b)}$$

Similarly equation (12) given by

$B_t + \xi q_x = 0$, where ξ is constant; can be rewritten by introducing a variable k such that $k \to q$ as $\varepsilon \to 0$ in $\frac{1}{\varepsilon}(k - \xi q)$, to have;

$$B_t + \xi k_x = 0 \quad \text{..... (23a)}$$

$$k_t + c_3^{\,2} B_x = \frac{1}{\varepsilon}(k - \xi q) \quad \text{..... (23b)}$$

If we let $\mathbf{u} = \begin{bmatrix} h \\ Q \\ B \end{bmatrix}$ and $\mathbf{v} = \begin{bmatrix} v \\ w \\ k \end{bmatrix}$ be vectors, then from equations (21) to (23),

$$\mathbf{u}_t + \mathbf{v}_x = 0 \quad \text{(24a)}$$

$$\mathbf{v}_t + \mathbf{C}^2\mathbf{u}_x = -\frac{1}{\varepsilon}(\mathbf{v} - \mathbf{F}(\mathbf{u}) - \mathbf{S}(\mathbf{u})) \quad \text{(24b)}$$

where $\mathbf{F}(\mathbf{u}) = \begin{bmatrix} Q & \frac{Q^2}{h} + \frac{gh^2}{2} & q \end{bmatrix}^T$

$$\mathbf{S}(\mathbf{u}) = \begin{bmatrix} 0 & -\int^x gh(y)B'(y)dy & 0 \end{bmatrix}^T$$

From equation (24) above $\mathbf{u},\mathbf{v} \in \mathbb{R}$ and $\mathbf{C}^2 \epsilon \mathbb{R}^{3x3}$ is a positive matrix. Here we assume without loss of generality that $\mathbf{C}$ has a positive eigenvalues $\mathbf{C}_j > 0$ for $j = 1,2,3$

System above can be formulated in vector matrix form as follows;

$$\begin{bmatrix} \mathbf{u} \\ \mathbf{v} \end{bmatrix}_t + \begin{bmatrix} 0 & \mathbf{1} \\ \mathbf{C}^2 & 0 \end{bmatrix} \begin{bmatrix} \mathbf{u} \\ \mathbf{v} \end{bmatrix}_x = \begin{bmatrix} 0 \\ -\frac{1}{\varepsilon}(\mathbf{v} - \mathbf{F}(\mathbf{u}) - \mathbf{S}(\mathbf{u}) \end{bmatrix} \quad \text{(25)}$$

The original sediment transport equations have now been replaced by a linear hyperbolic system with a relaxation source term which rapidly drives $\mathbf{v} \to \mathbf{F}(\mathbf{u})$ in the relaxation limit $\varepsilon \to 0$. In some cases it can be shown analytically that solution to system (25) approach solutions to the original equations. This is due to the convergence property that the characteristic condition is satisfied, whereby for system (25) every eigenvalue λ of $\mathbf{F}(\mathbf{u})$ satisfies $|\lambda| \le c_{\max}$, where $c_{\max} = \max_j c_j$.

By doing so we ensure that the characteristic speeds $c_{\max}$ of the hyperbolic part of system (25) are at least as large as possible as the characteristic speeds $|\lambda|$ of the original problem of the sediment transport equations before relaxation. Finally by choosing the constants c_1, c_2 and c_3 appropriately, so that the corresponding sub-characteristic conditions hold true, in the relaxation limit $\varepsilon \to 0$ we recover the original systems for relation (25).

b) SPATIAL DISCRETIZATION OF THE RELAXED SCHEME

We shall discretize the space first in the relaxed system (25) to obtain a semi-discrete system. We introduce the spatial grid points $x_{i+\frac{1}{2}}$ with mesh width $\Delta x = x_{i+\frac{1}{2}} - x_{i-\frac{1}{2}}$.

In carrying out this, the simplest way of modifying the piecewise constant data u_i^n is to replace the constant states u_i^n by a piece-wise linear function $u_i(x)$ in the first Godunov method, one assumes that u_i^n represent an integral average in the cell $I_i = x_{i+\frac{1}{2}} - x_{i-\frac{1}{2}}$ and is given by,

$$u_i^{\,n} = \frac{1}{\Delta x}\int_{x_{i-1/2}}^{x_{i+1/2}} u(x,t^n)dx \quad \text{..... (26)}$$

Now a piece-wise linear local reconstruction of u_i^n is

$$u_i(x) = u_i^{\,n} + \frac{x - x_i}{\Delta x}\Delta i \; ; \; x \in [0, \Delta x] \quad \text{..... (27)}$$

where in equation (27) above $\frac{\Delta i}{\Delta x}$ is suitable slope of $u_i(x)$ in the cell $I_i = x_{i+\frac{1}{2}} - x_{i-\frac{1}{2}}$ we can also call Δi a slope which can be chosen appropriately in order to make the scheme more accurate and u_i^n is defined locally in the cell, that is $x \in [0, \Delta x]$. The centre of the cell x_i in the local coordinates is $x = \frac{1}{2}\Delta x$ and $u_i(x) = u_i^{\,n}$. The values of $u_i(x)$ at the extreme points play a fundamental role; they are given by:

$$u_i^{\,L} = u_i(0) = u_i^{\,n} - \frac{1}{2}\Delta x \quad \text{..... (28a)}$$

$$u_i^{\,R} = u_i(\Delta x) = u_i^{\,n} + \frac{1}{2}\Delta x \quad \text{..... (28b)}$$

Equations (28a) and (28b) are gotten by substituting $x = 0,\ \mathrm{x_i} = \frac{1}{2}\Delta x$ and $x = \Delta x\ ,\mathrm{x_i} = \frac{1}{2}\Delta x$ respectively in equation (27) and are usually called boundary extrapolated values; hence the name variable extrapolated method. Note that the integral of $u_i(x)$ in the cell I_i is identical to that of u_i^n and thus the reconstruction process retains conservation. The following diagram illustrate piece-wise linear MUSCL reconstruction of data in a single computing cell. $I_i = x_{i+\frac{1}{2}} - x_{i-\frac{1}{2}}, x \in [0, \Delta x]$ and boundary extrapolated values are $u_i^{\,L}\ ,\mathrm{u_i}^{\,R}$

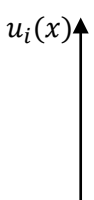

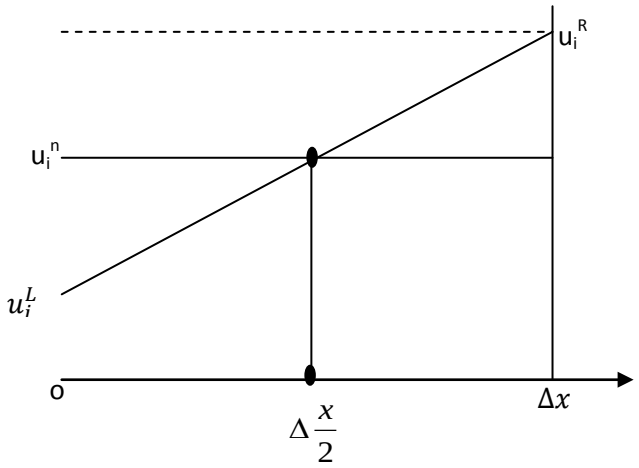

Figure 4: Piecewise linear MUSCL reconstruction of data in a single computing cell

Also considering piece-wise linear MUSCL construction of three successive computing cells I_{i-1}, I_i, I_{i+1} in the interval $I_i = \left[x_{i-3/2}, x_{i+3/2} \right]$,

we have

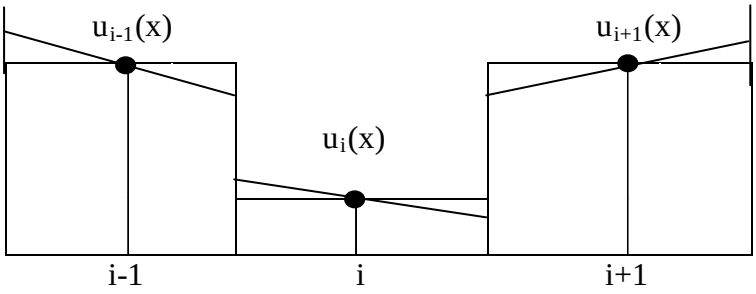

Figure 5: Piecewise linear MUSCL reconstruction of three successive computing cells

The diagram above illustrate the piecewise linear reconstruction process applied to three successive cells in the interval $I_i = \left[x_{i-3/2}, x_{i+3/2} \right]$ the data has been modified at each interface $i + 1/2$. MUSCL data reconstruction that are more accurate than the piecewise linear reconstruction are possible. For example a piecewise quadratic reconstruction is;

$$u_i(x) = u_i^{\,n} + \frac{x - x_i}{\Delta x}\Delta^{(1)} + \frac{3k}{2(\Delta x)^2}\{(x - x_i)^2 - \frac{(\Delta x)^2}{12}\}\Delta_i^{(2)} \quad \text{..... (29)}$$

where $\Delta_i^{(1)} = \Delta$ and $\Delta_i^{(2)}$ is the slope associated with the second derivative and k is the parameter.

The spatial discretization of equation (25) in conservative form can be written as

$$\frac{\partial}{\partial t}\mathbf{u}_i + \frac{1}{\Delta x}(\mathbf{v}_{i+\frac{1}{2}} - \mathbf{v}_{i-\frac{1}{2}}) = 0$$

$$\frac{\partial}{\partial t}\mathbf{v}_i + \frac{1}{\Delta x}\mathbf{C}^2(\mathbf{u}_{i+\frac{1}{2}} - \mathbf{u}_{i-\frac{1}{2}}) = -\frac{1}{\varepsilon}(\mathbf{v}_i - \mathbf{F}_i - \mathbf{S}_i)$$

where the average quantities $\mathbf{F}_i$ and $\mathbf{S}_i$ are defined by

$$\mathbf{F}_i = \frac{1}{\Delta x}\int_{x_{i-1/2}}^{x_{i+1/2}} \mathbf{F}(\mathbf{u})dx = \mathbf{F}[\frac{1}{\Delta x}\int_{x_{i-1/2}}^{x_{i+1/2}} \mathbf{u}dx] + o(h^2) = \mathbf{F}(\mathbf{u}_i) + o(h^2)$$

$$\mathbf{S}_i = \frac{1}{\Delta x}\int_{x_{i-1/2}}^{x_{i+1/2}} \mathbf{S}(\mathbf{u})dx = \mathbf{S}[\frac{1}{\Delta x}\int_{x_{i-1/2}}^{x_{i+1/2}} \mathbf{u}dx] + o(h^2) = \mathbf{S}(\mathbf{u}_i) + o(h^2)$$

for $\Delta x_i = \max \Delta x_{i.}$. Thus for sufficiently accurate spatial discretization we have $o(h^2)$ accuracy.

$$\frac{\partial}{\partial t}\mathbf{u}_i + \frac{1}{\Delta x}(\mathbf{v}_{i+\frac{1}{2}} - \mathbf{v}_{i-\frac{1}{2}}) = 0 \quad \text{.....} \quad \text{(30a)}$$

$$\frac{\partial}{\partial t}\mathbf{v}_i + \frac{1}{\Delta x}\mathbf{C}^2(\mathbf{u}_{i+\frac{1}{2}} - \mathbf{u}_{i-\frac{1}{2}}) = -\frac{1}{\varepsilon}(\mathbf{v}_i - \mathbf{F}_i - \mathbf{S}_i) \quad \text{.....} \quad \text{(30b)}$$

In equation (30a) and (30b) the point value quantities $\mathbf{u}_{i+\frac{1}{2}}$ and $\mathbf{v}_{i+\frac{1}{2}}$ will be defined by MUSCL schemes.

c) Flux limiter

Flux limiters are used in high resolution schemes, such as the MUSCL scheme to avoid the spurious oscillations (wiggles) that would occur with high order spatial discretization schemes due to shocks, discontinuities or sharp changes in the solution domain. Uses of flux limiter, together with an appropriate high resolution scheme make the solution Total Variation Diminishing (TVD). Various limiters have different switching characteristics and are selected according to the particular choices are

usually made on a trial and error basis. There so many limiters functions depending on their choices of accuracy; some of the most popular ones include.

Minmod slope (given as follows according to Roe 1986)

$$\phi(\theta) = \max(0, \min(1,0), \quad \text{..... (31a)}$$

$$\lim_{\theta\to\infty} \phi_{mm}(\theta) = 1.$$

Other forms of slope limiter functions include;

Monotonized central (MC) limiter function (Van Leer, 1977) given by

$$\phi(\theta) = \max[0, \min(\frac{(1+\theta)}{2}, 2, 2\theta)] \quad \text{..... (31b)}$$

$$\lim_{\theta\to\infty} \phi_{mc}(\theta) = 2.$$

This MC limiter function has also shown to exhibit sharper resolution of discontinuities since it does not reduce the slope as severely as Minmod (mm) near discontinuity. A sharper slope limiter as MC considered in this work was introduced by Van Leer (1974) and is given as;

$$\phi(\theta) = \frac{|\theta| + \theta}{1+\theta} \quad \text{..... (31c)}$$

with $\lim_{\theta\to\infty} \phi_{VL}(\theta) = 2.$

All the above limiters are symmetric because they exhibit the following symmetric property $\frac{\phi(\theta)}{\theta} = \phi(\frac{1}{\theta})$ this is a desirable property as it ensures that the limiting actions for forward and backward gradients operate on the same way .The above limiter functions are second order TVD. This means that they are designed such that they pass through a certain region of the solution. In order to guarantee stability of the scheme, second order TVD limiters satisfy at least the following criteria.

i. $\theta \le \phi(\theta) \le 2\theta, \quad (0 \le \theta \le 1)$

ii. $1 \le \phi(\theta) \le \theta, \quad (1 \le \theta \le 2)$

iii. $1 \le \phi(\theta) \le 2, \quad (\theta > 2)$

iv. $\phi(1) = 1$

For the scheme (31a) and (31b) to be TVD (when the lower order term is not present) a more general condition for ϕ is

$$0 \le \frac{\phi(\theta)}{\theta} \le 2 \text{ and } 0 \le \phi(\theta) \le 2 \quad \text{..... (31d)}$$

It has been shown (Van Leer) limiter function exhibits sharper resolution of discontinuities , since it does not reduce the slope severely as MM (1986) near a discontinuity , it should be noted here that MM provides sufficient bounds on the flux limiters for the TVD condition to be satisfied; but do not ensure second order accuracy (although the limiter used are second order) the following diagrams is an illustration of the limiter function mentioned above overlaid over onto second order TVD region.

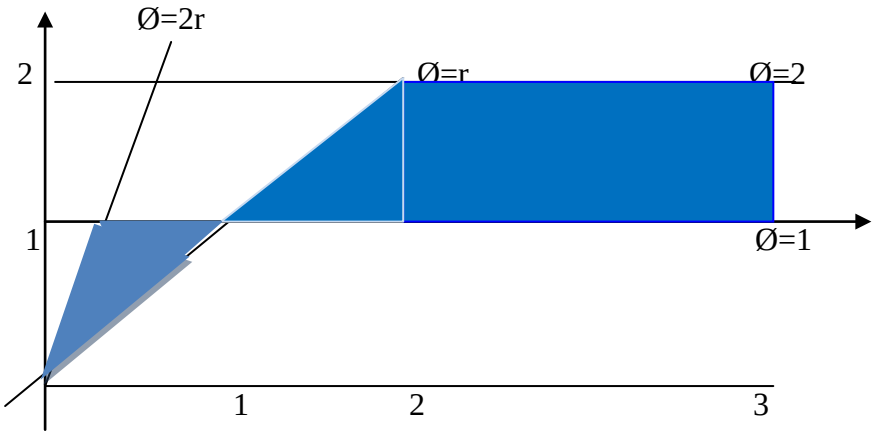

Figure 6: Admissible limiter region for second-order TVD schemes (Sweby, 1984)

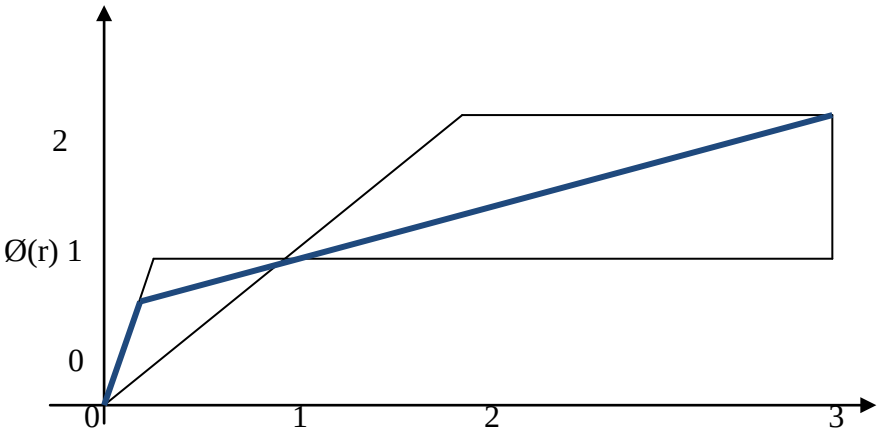

Figure 7: Minmod Limiter

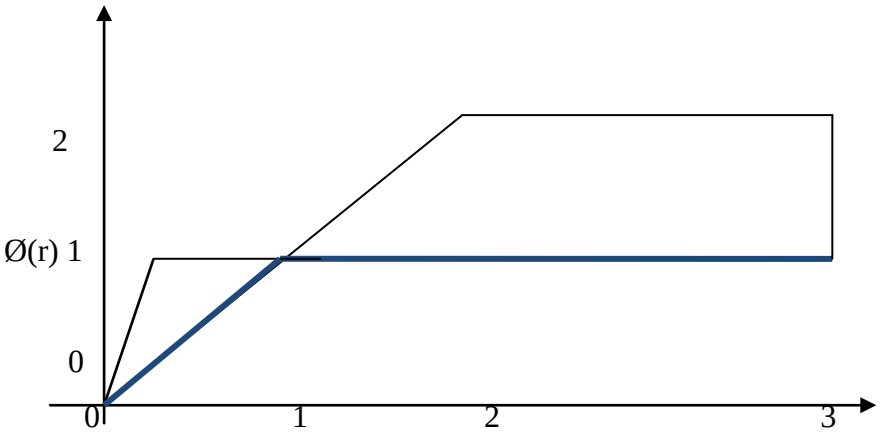

Figure 8: Monotonized Central Limiter

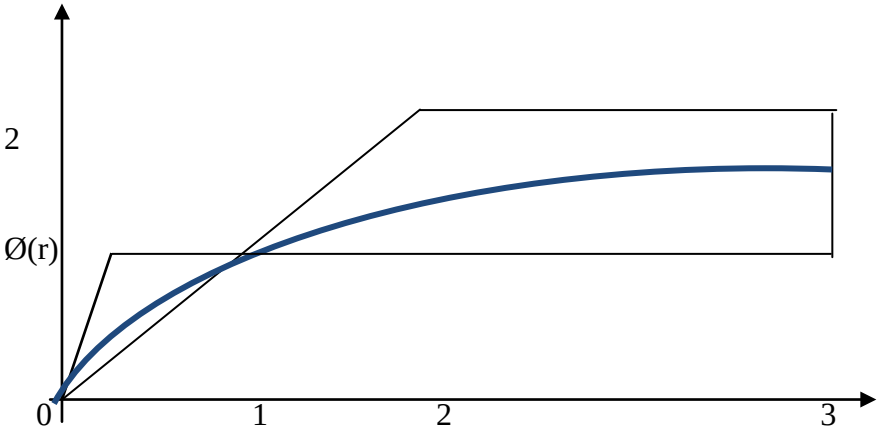

Figure 9: Van Leer Limiter

The three diagrams above illustrate how the Minmod, Monotonized central, and Van Leer limiter functions approximate the second order TVD regions (Sweby 1984). To obtain second order accuracy the function ϕ must pass smoothly through the point $\phi(1)=1$. In the above diagrams $v=\theta$, on x-axis and $\phi(v)=\phi(\theta)$ in y-axis. In the three diagrams above we have three limiters functions indicated by blue lines in the second order TVD region. The MC limiter has a fair approximation of the approximation of the discontinuity on the sharp point due to shocks within the flow; though the Minmod Limiter is not a good approximation since it deviates very far away from the point of shock. The most reliable and better limiter function is Van Leer. Since its approximation is within the second order region and it also takes the

shape of a curve as an approximation of the sharp corners due to shocks; it is therefore the one to be utilized in this work.

d) MUSCL – scheme

Van Leer (1979) introduced the idea of modifying the piecewise constant data

$$u_i^{\,n} = \frac{1}{\Delta x}\int_{x_{i-1/2}}^{x_{i+1/2}} u(x,t^n)dx$$

where u_i^n is the integral average of the solution $u(x,t^n)$ within the cell $I_i = \left[x_{i+\frac{1}{2}}, x_{i-\frac{1}{2}}\right]$ at a time $t = t^n$ and $\Delta x = x_{i+\frac{1}{2}} - x_{i-\frac{1}{2}}$ in the first order Godunov Method, as a first step to achieve higher order of accuracy. This approach is known as MUSCL or variable extrapolation method. MUSCL allows the construction of numerical methods that of very high order fully discrete or semi-discrete and also implicit. In our case we shall consider semi discretize case which will lead to an ordinary differential equation. The O.D.E shall be solved using an implicit second order Runge-kutta method since it works better than the Euler method. MUSCL approach implies high order of accuracy obtained by data reconstruction and reconstruction is constrained so as to avoid spurious oscillations. MUSCL-scheme is designed to preserve steady states as accurately as possible, again MUSCL relaxing scheme is particularly attractive because the solution remain stable, monotone and highly accurate without requiring special tracking techniques or deforming grids. Data reconstruction is performed on MUSCL scheme in order to increase the accuracy of the first order schemes and then apply the method in solving the vector-matrix equation (25).

To obtain this second order accuracy we use Van Leer`s flux limiter. This method does not use piecewise constant interpolation but instead it uses piecewise linear interpolation which applied to the p-th components of $v \mp cu$ gives respectively.

$$(v + c_p u)_{i+\frac{1}{2}} = (v + c_p u)_i + \frac{1}{2}\Delta x \Delta_i^{\,+} \quad \text{..... (32a)}$$

$$(v - c_p u)_{i+\frac{1}{2}} = (v - c_p u)_{i+1} - \frac{1}{2}\Delta x \Delta_{i+1}^{\,-} \quad \text{..... (32b)}$$

Here u, v are the p-th $(1 \le p \le 2)$ components of **u** and **v** respectively for the STEs, g is gravity constant, h and d are as shown above. $\Delta^{\pm}{}_i$ is the slope of the $v \mp cu$ on the ith cell. Using Sweby's notation the slopes of $\Delta^{\pm}{}_i$ ith cell is defined by.

$$\Delta^{\pm}{}_i = \frac{1}{\Delta x}(v_{i+1} \pm c_p u_{i+1} - v_i \pm c_p u_i)\phi(\theta_i^{\pm})$$

$$\theta_i^{\pm} = \frac{v_i \pm c_p u_i - v_{i-1} \mp c_p u_{i-1}}{v_{i+1} \pm c_p u_{i+1} - v_i \mp c_p u_i}$$

Solving equations (30a) and (30b) simultaneously gives;

$$v_{i+\frac{1}{2}} + c_p u_{i+\frac{1}{2}} = v_i + c_p u_i + \frac{1}{2}\Delta x \Delta_i^{+} \quad \text{(33a)}$$

$$v_{i+\frac{1}{2}} - c_p u_{i+\frac{1}{2}} = v_{i+1} - c_p u_{i+1} - \frac{1}{2}\Delta x \Delta_{i+1}^{-} \quad \text{(33b)}$$

Subtracting and adding the above respectively gives the values of $u_{i+\frac{1}{2}}$ and $v_{i+\frac{1}{2}}$

$$u_{i+\frac{1}{2}} = \frac{1}{2}(u_i + u_{i+1}) - \frac{1}{2c_p}(v_{i+1} - v_i) + \frac{\Delta x}{4c_p}(\Delta_i^{+} + \Delta^{-}{}_{i+1}) \quad \text{(34a)}$$

$$v_{i+\frac{1}{2}} = \frac{1}{2}(v_i + v_{i+1}) - \frac{c_p}{2}(u_{i+1} - u_i) + \frac{\Delta x}{4}(\Delta_i^{+} - \Delta^{-}{}_{i+1}) \quad \text{(34b)}$$

We solve for values of $u_{i-\frac{1}{2}}$ and $v_{i-\frac{1}{2}}$ by considering the results of equations (30a) and (30b)

$$u_{i-\frac{1}{2}} + c_p u_{i-\frac{1}{2}} = v_{i-1} + c_p u_{i-1} + \frac{1}{2}\Delta x \Delta_{i-1}^{+} \quad \text{(35a)}$$

$$v_{i-\frac{1}{2}} - c_p u_{i-\frac{1}{2}} = v_i - c_p u_i - \frac{1}{2}\Delta x \Delta_i^{-} \quad \text{(35b)}$$

Subtracting and adding respectively gives the values of $u_{i-\frac{1}{2}}$ and $v_{i-\frac{1}{2}}$

$$u_{i-\frac{1}{2}} = \frac{1}{2}(u_{i-1} + u_i) - \frac{1}{2c_p}(v_i - v_{i-1}) + \frac{\Delta x}{4c_p}(\Delta_{i-1}^{+} + \Delta^{-}{}_i) \quad \text{(36a)}$$

$$v_{i-\frac{1}{2}} = \frac{1}{2}(v_{i-1} + v_i) + \frac{1}{2c_p}(u_{i-1} - u_i) + \frac{\Delta x}{4}(\Delta_{i-1}{}^{+} - \Delta^{-}{}_i) \quad \text{..... (36b)}$$

Upon substituting equations (34b) and (36b) in (30a) and also (34a) and (36a) in (30b) we get

$$\frac{\partial u_i}{\partial t} + \frac{1}{2\Delta x}(v_{i+1} - v_{i-1}) - \frac{c_p}{2\Delta x}(u_{i+1} - 2u_i + u_{i-1}) - \frac{1}{4}(\Delta_{i+1}{}^{-} - \Delta_i{}^{-} + \Delta_{i-1}{}^{+} - \Delta_i{}^{+}) = 0$$

..... (37a)

$$\frac{\partial v_i}{\partial t} + \frac{c_p{}^2}{2\Delta x}(u_{i+1} - u_{i-1}) - \frac{c_p}{2\Delta x}(v_{i+1} - 2v_i + v_{i-1}) + \frac{c_p}{4}(\Delta_{i+1}{}^{-} - \Delta_i{}^{-} - \Delta_{i-1}{}^{+} + \Delta_i{}^{+}) = -\frac{1}{\varepsilon}(v_i - F_p(u_i))$$

$$-\frac{1}{\varepsilon}\bar{s}_p(u_i) \quad \text{.....(37b)}$$

$\bar{s}_p$ and F_p being the p th-components of $\bar{\mathbf{S}}_p$ and $\mathbf{F}_p$ respectively.

The two systems above (37a) and (37b) are the MUSCL for the relaxation system with source term. The fluxes on the spatial derivatives have been discretized leaving behind the time derivative. This system is an ODE and can be solved using TVD Runge-Kutta method since it works better than the Euler method in approximating time derivative.

e) Temporal discretization.

So far we have only discussed the spatial discretization. The semi-discrete scheme proposed above written in the conservative form

$$\frac{d}{dt}(Q_i(t) = \frac{F_{i+1/2}(t) - F_{i+1/2}(t)}{\Delta x} \quad \text{.....} \quad \text{(38)}$$

is a system of time –dependent ODEs for which many stable numerical solvers are known. The following focuses on the explicit Runge-kutta methods introduced by (shu and osher; 1988) which leads to step sizes under which the numerical process is TVD. An important feature of this class of time discretization is that they are convex combinations of first order forward Euler steps; hence they maintain strong stability properties in any semi-norm of the forward Euler step (shu 2003)

i) First order method

The first order Runge-Kutta temporal discretization is given by

$$Q^{n+1} = Q^n + \Delta t F(Q, t^n) \quad \text{..... (39)}$$

where

$F(Q_i, t^n) = F_{i+\frac{1}{2}} - F_{i-\frac{1}{2}}$ this algorithm is simple and computationally more efficient than any other higher order methods. However the first order accuracy of this approach is not consistent with the second order accuracy of this spatial discretization. For this reason it is important to consider second order temporal discretization.

ii) The second order method

$$Q_1^{\,n} = Q_i^{\,n} + \Delta t\, F_i^{\,n} \quad \text{..... (40a)}$$

$$Q_i^{\,n+1} = \frac{1}{2}Q_i^{\,n} + \frac{1}{2}Q_i^{(1)} + \frac{\Delta t}{2}F_i^{(1)} = \frac{1}{2}Q_i^{\,n} + \frac{\Delta t}{2}(F_i^{\,n} + F_i^{(1)}) \quad \text{..... (40b)}$$

This is also known as the improved Euler approximation. Simply this method produces an initial guess $Q^{(1)}$ to the solution at the next step and uses $Q^{(n+1)}$ to refine this guess.

f) Time discretization

The second order TVD Runge-kutta splitting scheme was introduced by (JIN 1995) that works very effectively for such problems. This splitting scheme takes two implicit stiff source steps and two explicit convection steps alternatively. In this section we present the time discretization of semi-discrete relaxation schemes to the STEs and this will finally give us a fully discrete scheme. We will see the space discretization MUSCL approach and applying an implicit Runge-kutta method as the time marching mechanism to advance them by one step Δt to simplify the presentation.

a) Given $\mathbf{u}^n, \mathbf{v}^n$ we apply a finite volume method to update $\mathbf{u}, \mathbf{v}$ over time Δt by solving the homogenous linear hyperbolic system.

$$\begin{bmatrix}\mathbf{u}\\ \mathbf{v}\end{bmatrix}_t + \begin{bmatrix}0 & 1\\ \mathbf{C}^2 & 0\end{bmatrix}\begin{bmatrix}\mathbf{u}\\ \mathbf{v}\end{bmatrix}_x = \begin{bmatrix}0\\ 0\end{bmatrix} \quad \text{..... (41)}$$

So we have $\frac{\mathbf{u}^{n+1}-\mathbf{u}^{n}}{\Delta t}=0\Rightarrow\mathbf{u}^{n+1}=\mathbf{u}^{n},\frac{\mathbf{v}^{n+1}-\mathbf{v}^{n}}{\Delta t}=0\Rightarrow\mathbf{v}^{n+1}=\mathbf{v}^{n}$ and obtain new values $\mathbf{u}^{(1)},\mathbf{v}^{(1)}$.

b) We again update $\mathbf{u}^{(1)},\mathbf{v}^{(1)}$ to $\mathbf{u}^{(n+1)},\mathbf{v}^{(n+1)}$ by solving the equations

$$\mathbf{u}_t=0 \quad \text{..... (42a)}$$

$$\mathbf{v}_t=-\frac{1}{\varepsilon}(\mathbf{v}-\mathbf{F}(\mathbf{u})-\mathbf{S}(\mathbf{u})) \text{ Over time } \Delta t \text{ ..... (42b)}$$

For the source term application corresponding to system (25) and temporally dropping the subscript indices i since we are dealing only with the derivative, then we can compute $\{\mathbf{u}^{n},\mathbf{v}^{n}\}$ and $\{\mathbf{u}^{n+1},\mathbf{v}^{n+1}\}$ as follows.

Taking into consideration equations (43a) and (43b),

$$\mathbf{u}^{n,1}=\mathbf{u}^{n} \quad \text{..... (43a)}$$

$$\mathbf{v}^{n,1}=\mathbf{v}^{n}+\frac{\Delta t}{\varepsilon}(\mathbf{v}^{n,1}-\mathbf{F}(\mathbf{u}^{n,1}))+\frac{\Delta t}{\varepsilon}\mathbf{S}(\mathbf{u}^{n,1}) \quad \text{..... (43b)}$$

The fully discretized scheme is obtained by advancing time marching mechanism as follows;

For the 1st implicit step, we obtain,

$$\mathbf{u}^{(1)}=\mathbf{u}^{n,1}-\Delta t\, D_{+}\mathbf{v}^{n,1} \quad \text{..... (44a)}$$

$$\mathbf{v}^{(1)}=\mathbf{v}^{n,1}-\Delta t\,\mathbf{C}^{2}D_{+}\mathbf{u}^{n,1} \quad \text{..... (44b)}$$

For the 1st explicit step, we obtain,

$$\mathbf{u}^{n,2}=\mathbf{u}^{(1)} \quad \text{..... (45a)}$$

$$\mathbf{v}^{n,2}=\mathbf{v}^{(1)}-\frac{\Delta t}{\varepsilon}(\mathbf{v}^{n,2}-\mathbf{F}(\mathbf{u}^{n,2}))-\frac{2\Delta t}{\varepsilon}(\mathbf{v}^{n,1}-\mathbf{F}(\mathbf{u}^{n,1}))-\frac{\Delta t}{\varepsilon}\mathbf{S}(\mathbf{u}^{n,2})-\frac{2\Delta t}{\varepsilon}\mathbf{S}(\mathbf{u}^{n,1})$$
..... (45b)

For the 2nd implicit step, we obtain,

$$\mathbf{u}^{(2)}=\mathbf{u}^{n,2}-\Delta t D_{+}\mathbf{v}^{n,2} \quad \text{..... (46a)}$$

$$\mathbf{v}^{(2)} = \mathbf{v}^{n,2} - \Delta t\, \mathbf{C}^2 D_+ \mathbf{u}^{n,2} \quad \text{..... (46b)}$$

For the 2nd explicit step, we obtain,

$$\mathbf{u}^{n+1} = \frac{1}{2}(\mathbf{u}^n + \mathbf{u}^{(2)}) \quad \text{..... (47a)}$$

$$\mathbf{v}^{n+1} = \frac{1}{2}(\mathbf{v}^n + \mathbf{v}^{(2)}) \quad \text{..... (47b)}$$

where we have defined the difference operator

$$\mathrm{D}_+ \mathbf{w}_i = \frac{1}{\Delta x}(\mathbf{w}_{i+\frac{1}{2}} - \mathbf{w}_{i-\frac{1}{2}})$$

The idea of keeping the convection terms explicit has great advantages here. First, does not need to solve systems of linear algebraic equations that will arise if the convection terms are implicit. Secondly, and more importantly due to the special structure of the source term, one does not need to solve any systems of nonlinear algebraic equations, despite of the nonlinear source terms. As a matter of fact one can always update u from the first equation, applying it to F (u) then solving the second equation to v exactly, since v is linear in the relaxation system.

Since the source terms are treated implicitly this time discretization is stable independent of ε given that the CFL condition from the convection is satisfied that is, the time discretization in the limit when $\varepsilon \to 0$ converges to the TVD Runge-Kutta schemes is given in Shu and Osher (1988).

Remark: note that equation (43b) is consistent to the relaxation systems due to a negative parameter it will break down if $\Delta t = 0(\varepsilon)$ .However, here we are developing under resolved numerical methods in the regime that $\Delta t >> \varepsilon$ thus equation (43b) will never break down in our case (JIN and XIN 2002). CFL conditions must be considered to ensure the stability is maintained in the interpretation of the results.

In all the calculations we have used $C_{cfl} = 0.5$, $\mathrm{S}_{\max}(\eta) = 19$ and relaxation rate $\varepsilon = 10^{-8}$ (Delis and Papoglou 2007).

V. NUMERICAL RESULTS AND DISCUSSION .

Numerical results and discussion for bump

In this test case, the small bump in the riverbed is interacting with the water flow where the water is moving slowly. Since the dimensionless parameter A and porosity σ determines the changes of bed; we can relate the two, as follows.

$A = f(\sigma) = A_0\sigma^3$ where $A_0 = 2$

We will show and compare the evolution of bed and the waves on the water surface for porosities 0.3 and 0.6.

Initial conditions

$h_L = h_R = 1$

$(hu)_L = (hu)_R = 0.0005 \approx 0$

$B(x,0)$ is specified using the normal distribution function

$(normdf(x,50,5))$ where $0 \le x \le 100$, 50 and 5 being the mean and variance respectively.

Case 1: porosity of 0.3

In this case, the blue colour profile represent the bump for bed of zero porosity (no eroding) while the black continuous profile the bump for bed of porosity 0.3 and the black broken profile the behavior of the water surface.

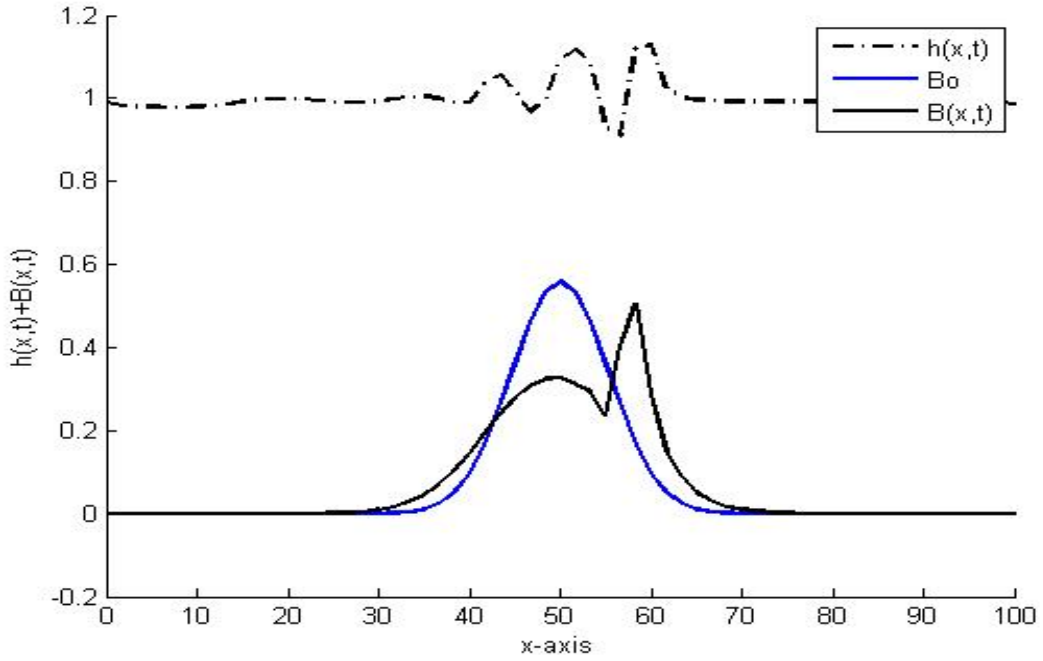

Figure 10: Numerical solution of bump for B+h $(\sigma = 0.3)$

The initial bump (blue in colour) which is specified using normal distribution is taken to have a porosity of zero and therefore no eroding of bump. When the porosity is increased to 0.3 the bump erodes and its bed height (B) reduces significantly especially at the mean (x=50). The eroded sediment is deposited immediately after the bump. As the flow interacts with the bump, there is formation of the water waves on the surface of the flow. This suggests that one of the factors that dictate eroding is the porosity of the sediment.

Case 2: porosity of 0.6

In this case, the blue colour profile will represent the bump for bed of zero porosity (no eroding) while the red continuous profile the bump for bed of porosity 0.6 and the red broken profile the behavior of the water surface.

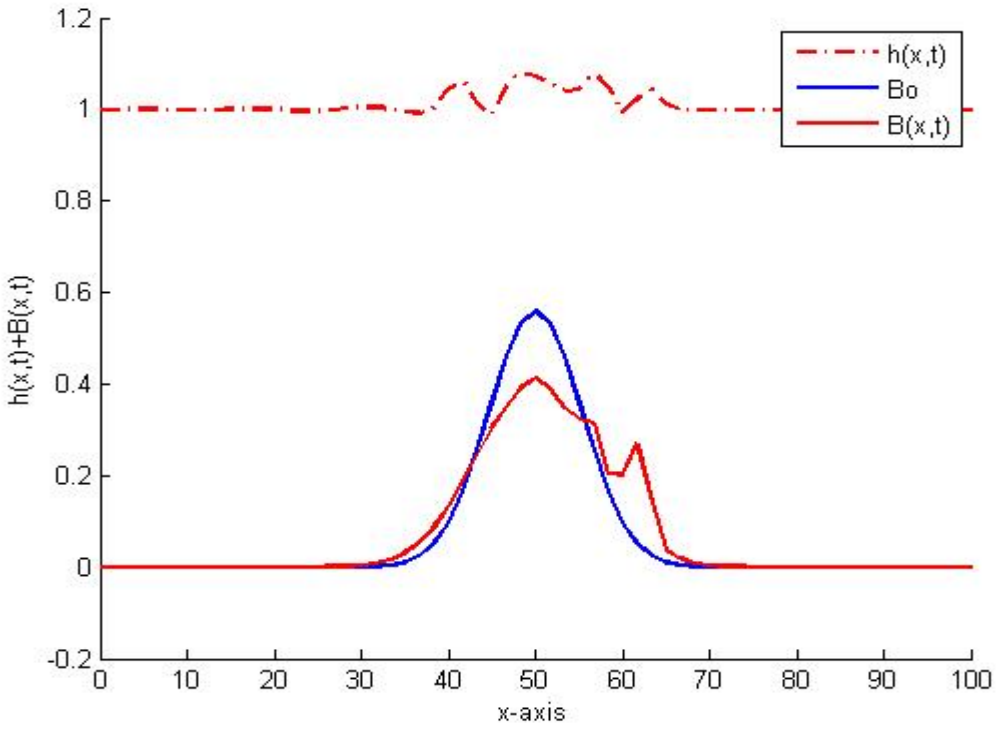

Figure 11: Numerical solution of bump for B+h $(\sigma = 0.6)$

When the porosity is increased to 0.6 there is rampant interaction between the flow and the sediment and therefore the bump erodes even more and consequently there is more deposition of sediments .The bed height reduces even further. As the flow interacts with the bump, still there is formation of water waves on the surface of the flow. This signifies that as the porosity increases so the rate of eroding and deposition.

Case 3: For three bed evolutions (porosities 0, 0.3 and 0.6)

In this case, the blue colour profile will represent the bump for bed of zero porosity (no eroding) while the black profile the bump for bed of porosity 0.3 and the red profile the bump for bed of porosity 0.6.

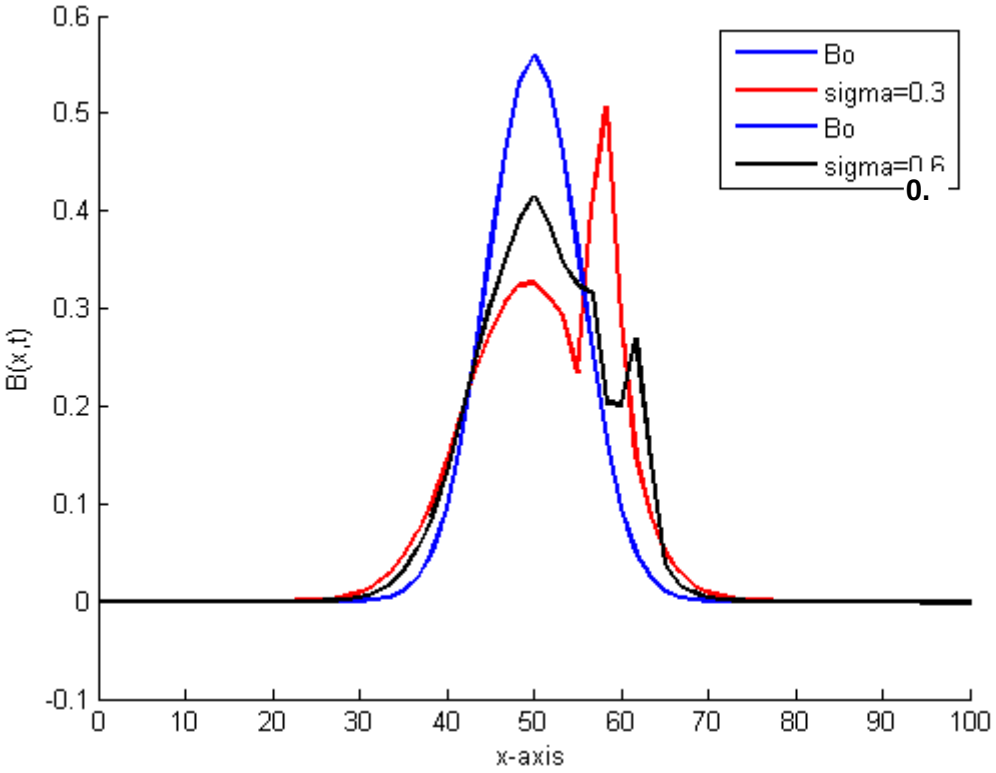

Figure 12: Bed height comparison of bump for porosities 0, 0.3 and 0.6

Comparing the beds for porosities 0, 0.3 and 0.6 it can be seen that as you increase the porosity there is more eroding of the bump hence reducing the bed height (B) and consequently increasing the water height (h). Still it can be noted that, as the bump erodes more there is more deposition of the sediments. This confirms that the rate eroding is a function of porosity.

Numerical results and discussion for trench

In this case the small trench on the river runaway is interacting with the water flow .The velocity of the water flow is determined by the height (h) of the river; the greater the height, the higher the velocity.

Like the test problem one the constant dimensionless parameter A and porosity σ determines the changes of the bed; we can relate the two as follows;

$$A = f(\sigma) = A_0\sigma^3 \text{ where } A_0 = 2$$

In this case we will show the entrainment and deposition of sediments for porosity 0.3 and 0.6 for water flow interacting quickly with the bed.

Initial conditions

$h_L = 1.2, \quad h_R \equiv B_0 = 0.2$

$B_0 = 0.2 \quad \forall x$

$(hu)_L = (hu)_R = 0.0005 \approx 0$

Case 1: Entrainment and Deposition for porosity 0.3

In this case, the black continuous profile depicts the initial bed surface at zero porosity and the entrainment and deposition for bed porosity 0.3, while the black broken profile depicts how the water waves are formed on the surface at 0 and 0.3 porosities.

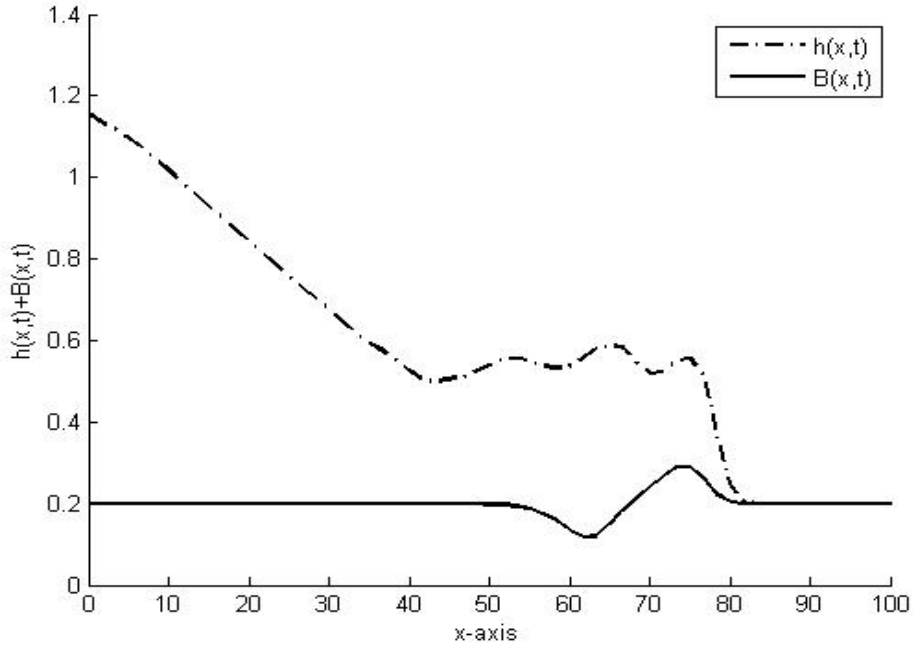

Figure 13: Numerical solution of trench for B+h ($\sigma = 0.3$)

Discussion of Case 1

When the flow approaches the region with porosity 0.3 the sediment is eroded leaving an entrainment. The eroded sediments are deposited immediately after the formation of the trench. As the flow interacts with the trench, still there is formation of water waves on the surface of the flow. In this case there is quick interaction between the flow and the sediment and hence the computational time is much reduced.

Case 2; Entrainment and Deposition for porosity 0.6

In this case, the red continuous profile depicts entrainment and deposition for bed porosity 0.6, while the red broken profile depicts how the water waves are formed on the surface for bed porosity 0.6.

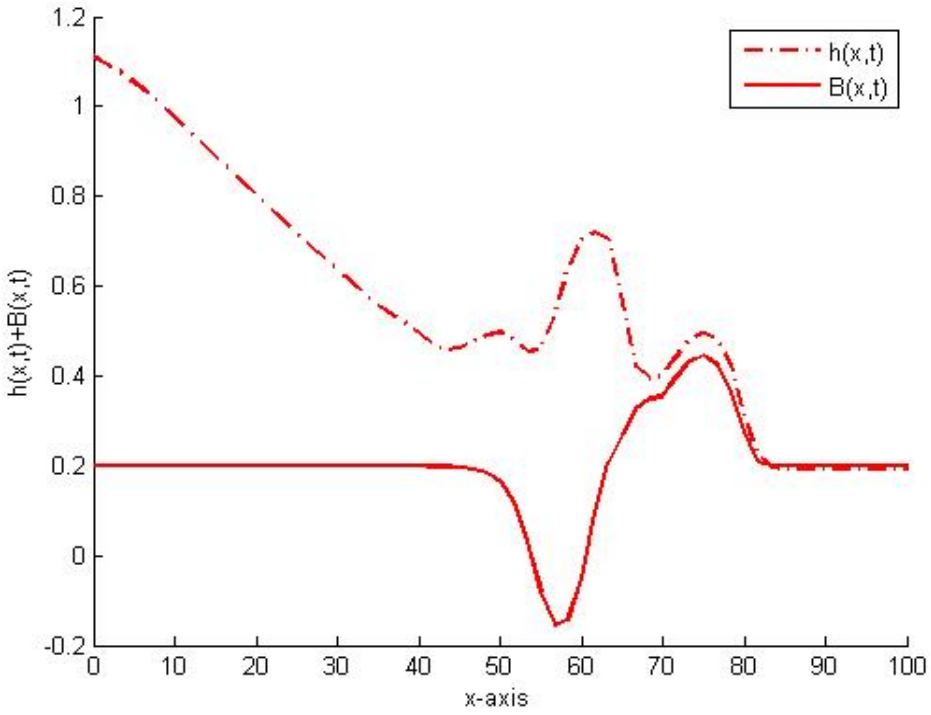

Figure 14: Numerical solution of trench for B+h (porosity 0.6)

Discussion of Case 2

When the porosity is increased to 0.6 the entrainment and deposition increases more. Still the water waves on the surfaces also become rampant. This shows that, as the porosity increases so the rate of entrainment and hence the deposition.

Case 3: Entrainment and Deposition for porosities 0, 0.3 and 0.6

In this case, the blue colour profile represent zero porosity with no eroding, while the black and red represent the entrainment and deposition of porosities 0.3 and 0.6 respectively.

Figure 15: Bed height comparison of trench for porosities 0, 0.3 and 0.6

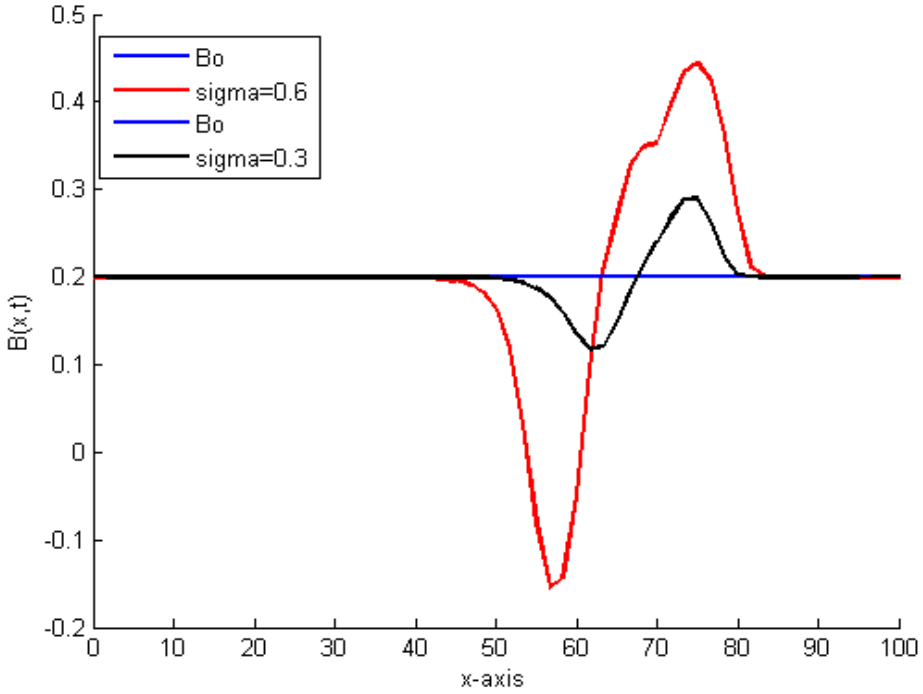

Discussion of Case 3

Comparing the three different porosities of the sediment, it can be seen that as the porosity increases, there are subsequent increase of entrainment and deposition. The bed height increases as the porosity increases, therefore the formation of entrainment and deposition of sediment is determined by the porosity of the bed.

V. CONCLUSION

The main objective of the study was to study how porosity and sediment transport changes the bed topography and water surface. In this work we have focused on the development and performance of a numerical relaxation approximation to the bed-level sediment transport in one space dimensions. Relaxation heme has been successfully utilized to analyze numerically the hyperbolic shallow flows, sediment

transport and bed evolution. The main feature of the scheme is its simplicity and robustness. MUSCL scheme (second order) which is finite volume shock capturing spatial discretization that is Riemann solver free has been used together with Van Leer flux limiter, providing accurate shock resolution.

In all the test cases presented in C- formulation they produced stable nonoscillatory results that are in agreement with those produced by modified second order Roe-type scheme (Hudson.2001). In the two test problems used, we realize that the porosity is one of the key factors that control erosion in soils and in rocks and therefore it should be a basic factor to consider when doing agriculture, transport of solute, assessment of permeability, construction of dams and so on.

REFERENCES

Banda, M.K and Seaid (2005), *Higher – order relaxation schemes for hyperbolic systems of conservation laws.*

Cunge, J.A and Holly F.M (1980), Practical *Aspects of computational River Hydraulics*, Pitman, London.

Delis, A.I and KatsaounisTh (2003), *Relaxation schemes for the shallow water equations*; int. J. Numer. Meth Fluids 41 695-719.

Delis, A.I and Katsaounis Th. (2004), *A generalized relaxation Method for Transport and diffusion of pollutant models in shallow water*, Comp. Methods. APPL. Math.4 410-430.

Delis, A.I and papoglou (2007), *Relaxation approximation to bed-load sediment transport.*

Dung, N.V *et al* (2014), *Large scale suspension sediment transport and sediment deposition in the Mekong Delta.*

Glaister, P (1987), *Difference Schemes for the Shallow Water Equations, Numerical Analysis Report*9/97, University of Rea.

Godunov, S.K (1959), *A Finite Difference Method for the computation of discontinuous solutions of the equations of fluid dynamics.*

Hudson, J (2001), *Numerical techniques for morphodynamic modeling*, PhD.Thesis, university of Reading.

Hudson, J, and Sweby P.K (2003), *Formulations for numerically approximating hyperbolic systems governing sediment transport*, J. Sci. Comp. 225-252.

Jin, S and Levermore C.D, *Numerical schemes for hyperbolic systems with stiff relaxation terms*, J .Comp. Phys, submitted.

Jin, S. and Xin (1995), *The relaxing schemes of conservation laws in arbitrary space dimensions*, comm. pure. Math 48.

Katsaounis, et al, (2001), *Adaptive Finite Element Relaxation Schemes for Hyperbolic Conservation Laws.* ; 35:17-33.

Lax, P.D *et al*. (1983), *On Upstream differencing and Godunov-type schemes for hyperbolic conservation laws*. SIAM Rev 35-61.

LeVeque, R.J (1992), *Numerical methods for conservation Laws* ,Birkhauser

Li, S. and Duffy C.J (2011), *Fully coupled approach to modeling shallow water flow, sediment transport and bed evolution in rivers Water Resource* 47, W03508,doi; 10.1029/2010WR009751.

Liggelt, J.A (1994*), Fluid Mechanics*. McGraw Hill, Inc.

Liu, T.P (1987), *Hyperbolic Conservation Laws with relaxation*, comm.mathsphys 108.

Rijn, L.C (1984), *Sediment Transport: Part I: Bed Load Transport; Part II:Suspended Load Transport; Part III: Bed Forms and Alluvial Roughness*, Proc.ASCE Journal of Hydraulics Division, Vol 110, HY10, 1431-1456; HY11, 1613-1641; HY12, 1733 – 1754.

Rijn, L.C (1993), Principles of Sediment Transport in Rivers, Estuaries and Coastal Areas, Aqua publications.

Rijn, L.C (1995), *Principles of sediment Transport in rivers, estuaries and coastal areas*, Aqua publications.

Shi and Xin (2002), *The Relaxation Schemes for systems of conservation Laws in Arbitrary Space Dimensions.*

Shu, C.W and Osher S (1988*), Efficient Implementation of essentially non-oscillatory shock capturing schemes*, J. Comp 77 439-471.

Soulby, R.L (1997), *Dynamics of Marine sands*; a manual for practical applications.

Sweby, P.R (1984), *High resolution Schemes using flux limiters for hyperbolic conservation laws*, SIAM.J. Num. Anal 21,995-1011.

Toro, E.F. (2001), *Riemann Solvers and Numerical Methods for Fluid Dynamics.*

Vveugddenhil, C.B (1994), *Numerical Methods for Shallow –Water flows.*